Signal Processing Opportunities and Challenges Towards Radar-on-Chip/in-Package in Autonomous-Driving Vehicles and Intelligent Transport Systems

Sergio Saponara, *IEEE Senior Member*, Maria Sabrina Greco, *IEEE Fellow*, Fulvio Gini, *IEEE Fellow*

Dept. Information Engineering, University of Pisa, via G. Caruso 16, 56122, Pisa, Italy

Abstract

This survey paper addresses the signal processing challenges for the design of radar-on-chip/in-package in the autonomous driving era, taking into account recent integration trends and technology capabilities. Radar signal processing platform specifications are discussed, and the radar sensor is compared to other competing sensors, such as Lidars and ultrasonics and video cameras, that aim at detecting still or moving objects too, and at measuring their motion parameters. This survey paper first focuses on signal processing techniques to be used for a cheap and power-efficient radar sensor, which operates in real-time while ensuring the automotive coverage-range needs. The main signal processing techniques for velocity-range estimation, direction estimation, waveform design and beamforming are analyzed, with particular emphasis on the radar physical layer co-design. Exploiting future evolution of embedded computing platforms, advanced signal processing techniques are enabled such as Multi-Input Multi-Output and cognitive radars, with adaptive waveforms to solve interference and spectrum scarcity issues.

Keywords: Radar-on-chip signal-processing; Radar sensing for autonomous driving; Embedded signal processing

I. Introduction

Intelligent transportation systems for surveillance and assisted/autonomous driving require robust sensing platforms, tolerant to bad light and weather conditions [1, 2]. This is a topic of high economic and societal impact, since every year 1.25 millions of people die worldwide due to accidents. Moreover, each year 90 millions of vehicles are sold, and hence a market valued at well over hundreds of billions of United States Dollars (USD) is potentially available for adoption of radar as a ubiquitous mobility sensor. In that respect, due to the emerging scenario of autonomous vehicles [3, 4], with alliances among traditional OEM (Original Equipment Manufacturer) or Tier-1 (e.g. BMW, VW-Audi, Toyota, FCA, Daimler, GM, Ford, Bosch, Denso, Continental, Valeo, MagnetiMarelli, etc.), and

new companies investing in vehicular technologies (Intel, Google-Waymo, Uber, Tesla, etc.), the interest in low-cost, compact and energy-efficient radar signal processing techniques is further increasing.

In the last years, the design of ubiquitous radars, available with low cost and low power in a large volume market as System-in-Package solution (SiP), is becoming feasible [5-9]. This is mainly due to the recent advances in i) in–package antenna array design, ii) integration as a System-on-Chip (SoC) of multi-channel RF transceivers and high performance Analog to Digital Converters (ADC), iii) embedded high performance computing (HPC) and memory platforms that enable advanced signal processing techniques to be implemented in real-time and with low power cost.

Fig. 1: Multi-vehicles scenario, all equipped with multiple remote sensors and connected with V2V/V2I links[1]

Intelligent transport systems (ITS) involve two main usages of radars, see Fig. 1:

- For **surveillance,** where radar sensors are embedded in the infrastructure to increase the safety of railroad crossing, urban crossing, parking areas [10] or for traffic flow analysis [11].

- For **vehicles' perception,** where radar sensors are mounted on-board vehicles to enable high levels of autonomy in assisted/autonomous driving [5].

Many signal processing review works have been proposed in the literature for automotive radar, but most of them propose a review of basic signal processing techniques [2-4, 12], considering the scenario of a car moving in multi-

[1] scenario adapted from https://blogs.intel.com/iot/2015/11/23/building-the-next-generation-car-with-intel-iot/

target scenario and equipped with pulsed or FMCW (Frequency Modulated Continuous Wave) radar. Such surveys are missing the analysis of implementation technology capabilities and trends, and that of advanced techniques, like cognitive radar signal processing. Indeed, when vehicles and ITS are moving from assisted to autonomous driving, the application scenario will be that of Fig. 1. It corresponds to the last 3 levels out of 6 in the SAE (Society of Automotive Engineers) classification of assisted/autonomous driving [5], moving from L0 (full human and manual control of all aspects of driving) to L5 (full autonomous driving), being L1, L2, L3 and L4 intermediate levels of assisted or autonomous driving. Such scenario foresees multiple vehicles, all equipped with multiple on-board remote sensors (radars, cameras, ultrasonics, Lidars), connected to each other and with the infrastructure with V2V/V2I (Vehicle-to-Vehicle, Vehicle-to-Infrastructure) communication technologies. The needs of real-time and low-latency perception and decision-making, of a continuous adaption to the sensed environment, of overcoming mutual-interference and spectrum scarcity issues, require cognitive radar signal processing solutions. Cognitive radar signal processing has been recently discussed in [13, 14 and references therein], but without any reference to its cost, power and time budgets, in order to be suitable for real implementation on-board vehicles. Moreover, mixing active and passive radar signal processing technologies can help reducing spectrum scarcity and electromagnetic (EM) interference. Several opportunities to solve the above issues come from the recent advances in SoC and SiP integration capabilities that are reviewed in this survey paper. This work considers both the scenarios of embedded signal processing for cheap and power-efficient radar sensor nodes and that, needing HPC, of cognitive and multi-sensor perception systems, using active and passive technologies. Hence, this paper is companion of [15, 16], published in this same special issue, focused more on the many new signal processing techniques for automotive radars. The intent of this paper is to review already implemented and new radar signal processing algorithms in light of existing and prospective technology solutions and capabilities.

After the description of the motivation, significance of the topic and evolution of this R&D field, this survey paper is organized as follows. Sect. II reviews the state-of-the-art of mobility sensors and radar on-chip/in-package specifications. This section focuses on known radar sensing systems, considering both commercial proposed solutions and recent R&D initiatives. Integration trends and technology capabilities (of antenna arrays, of multi-channel mmWave radar transceivers and high-speed ADC, of embedded HPC and memory) are analyzed and the radar sensors compared to other competing sensors, such as Lidars and ultrasonics and video cameras, that aim at detecting still or

moving objects too, and at measuring their motion parameters. Once defined in Sect. II the radar signal processing platform specifications, the signal processing challenges for the design of a radar-on-chip/in-package in the autonomous driving era are described in two dedicated sections, Sect. III and Sect. IV. The first section is focused more on which signal processing techniques have to be used to have a radar sensor cheap, power-efficient, and operating in real-time, while ensuring the automotive coverage-range needs. Sect. III provides more details about the main signal processing techniques (velocity-range estimation, direction estimation, waveform design, beamforming, etc.) implemented in radar-on-chip systems, with particular emphasis on the radar physical layer co-design. Limits and opportunities for real-time implementable signal processing techniques are discussed, considering trends in the design of scalable and energy-efficient mixed-signal front-end, embedded HPC and memories, based on SoC or Field-Programmable SoC (FPSoC). Instead, Sect. IV exploits future evolution of embedded HPC platforms focusing on advanced signal processing techniques such as MIMO (Multi-Input Multi-Output) and cognitive radars. Sect. V summarizes main conclusions of this paper and traces a path for future work.

II. Review of state-of-art of mobility sensors and radar-on-chip/in-package specifications

As shown in Fig. 1, the sensing technologies competing at the state-of-art with radars to detect the presence of a target and to measure its distance, motion direction, and speed, are mainly Lidars and video cameras. Ultrasonic technology, thanks to its maturity and low-cost, is adopted too, but limited to the use as an array of multiple devices for short range (<1 m) detection of vehicle surrounding obstacles in low-speed urban scenarios.

Lidar is an active sensor, which allows measurements of distance with high resolution and speed. However, Lidars are heavy and costly sensors. For instance, the LMS 291 in [17] has a weight of 4.5 Kg and a power consumption of 20 W from a 24V DC supply. The HDL-32E has lower weight [18], 1.3 Kg, and lower power consumption, 12 W. The cost of today commercial available Lidars [17, 18] for autonomous driving ranges from few thousands to tens of thousands of USD. The cost of a Lidar sensor is one of the main bottleneck for widespread adoption of this technology on-board vehicle and, as discussed in [5], there are several initiatives in industry to reduce it. For example, MEMS (micro electro mechanical system) micro-mirror technology can be used to reduce the cost of 3D scanning Lidars, this technology is still in its infancy.

Arrays of video cameras and/or ultrasound sensors and/or infrared sensors have been proposed in [19] for obstacle detection. They allow low-cost and low-power recognition and classification of targets, thanks to the evolution of

CMOS camera–on-chip technology. However, the detection range and the measurements of distance and speed with video cameras is typically limited to tens of meters. Therefore, applications are limited to parking assistance of cars or obstacle detection at low speed in crowded urban traffic. Moreover, camera sensors operating in the visible spectrum are not robust in case of bad weather and bad light conditions. By adding also thermal cameras, operating in long-wave infrared (LWIR) spectrum range, wavelength from 7 to 14 μm, thus creating a multi-camera multi-spectral system, the detection and measurement activities became more robust to bad operating conditions (e.g. sun glares, low light, fog). However, the maximum covered range is still limited to tens of meters and the increased robustness is paid in terms of increased cost (thousands of euros for multi-spectral video measuring systems including a LWIR camera, although with a limited 640x480 pixel resolution).

Radars are less sensitive to weather conditions, allowing for a safe detection of obstacles during heavy rain, snow, and hail, in presence of dense fog, strong sun glares, and environmental noises and vibration. Radar sensing is also preferable to non-imaging technologies, like induction loops and photoelectric or RF interruption beam sensors, due to its relatively small size and its easier installation, use and maintenance.

Low-cost and low-power radars have been proposed recently, such as the 60 GHz radar in [20], for proximity detection, or low-power Ultra-Wide Band (UWB) radar sensors, for measuring vital signs in [21], which can be useful for driver health and attention status in assisted driving systems. However, in the above cases, the covered range is limited to a few meters, and hence the sensors are not suited neither for land or maritime transport surveillance applications nor for autonomous driving in extra urban or highway scenarios.

For transport surveillance radar, when monitoring a railroad crossing, or a road crossing, or a parking, the needed detection range is on the order of hundreds of meters. Extending the requirement to maritime applications such as monitoring harbor ingress/egress traffic [22] the range distance to be covered is above 1 Km. The use for transport applications lead to severe requirements in terms of both harsh operating conditions and functional safety. A safety integrity level (SIL) 4 is often required with an acceptable fault rate below 10 FIT (Failure in Time), where 1 FIT means maximum 1 failure each 10^9 hours of operation, and a diagnostic of faults with a rate higher than 99%.

Many works on low-cost and low-power radars have been proposed in recent literature from academia and industry. For example, STARS-railway systems [23], a new joint venture company of IDS and INTECS, proposed radar-based solutions for the automatic detection of objects which have fallen on railway tracks in high-risk zones (i.e. near

overpasses, tunnels and areas prone to landslides) or for the prevention of train collisions with obstacles on the track at level crossings. To this aim, a network of multiple X-band FMCW radars is used, each exploiting microwave COTS (Commercial Off The Shelf) board for the front-end and FPGA (Field Programmable Gate Array)-based radar signal processing [24].

For perception use in autonomous-vehicles (automotive and drone/robotics applications), electronic companies like Bosch, Denso, or Continental, to name just a view, have proposed several types of short-range and low-range mmWave Radars (operating at 22-24 GHz in [25], or at 77-79 GHz in [26], 80 GHz in [27], 90 GHz or above in [28]). However, there is a trade-off between Field of View (FoV) and distance with maximum detection range limited to 250 m at a very narrow FoV, or at less than 10 m for large FoV. Moreover, the detection accuracy in distance, angle and speed is still not enough for fully autonomous driving where cm-accuracy is required. Although estimation algorithms like ESPRIT, MUSIC or RELAX are available in the literature [29, 30], their cost-effective and real-time implementation in automotive radar is still to be achieved. Problems like interference with other V2V/V2I RF signals [31-33], privacy/security, low EM emissions, data fusion with other sensors, have still to be solved.

To improve resolution and SNR performance, MIMO schemes may be applied in automotive radar [22, 24, 34-37]. In a MIMO radar, a critical design issue is the optimal placement of transmitting and receiving arrays. For example, the series-production radar in [36] has two transmitting antennas, with 5.32 cm spacing, and six receiving antennas, with 8.9 mm spacing. Indeed, the physical position of the transceivers affects directly the properties of the virtual array. The radar system in [37] for urban environments has up to 16 transmitting antennas, working simultaneously, and 16 receiving antennas, each one with dedicated ADC and processing channel using commercial GaAs-based monolithic microwave integrated circuit (MMIC) with 77 GHz carrier and 2 GHz bandwidth. In literature, research on genetic algorithms to search for the optimal antenna placement has been carried out (see e.g. [38]). An integrated SiGe time-division-multiplexing MIMO radar sensor for the 76-81 GHz frequency band was presented in [39], using dielectric lens antennas (4 array of patch antennas integrated on the board).

Increasing the integration capability will enable new opportunities for radar signal processing. As discussed in [7-9], radar integration technology has moved from using costly GaAs discrete MMIC, e.g. the 2nd generation Long Range Radar (LRR2) from Bosch, to Silicon-integrated mmWave circuits with SiGe BiCMOS in the 3rd and 4th generation. This allowed increasing the complexity of the embedded radar techniques, increasing the number of in-package

antennas (from 4 to 6), increasing the accuracy level, from LRR2 accuracy of 50 cm, to better than 10 cm in LRR4 (4^{th} generation Long Range Radar). The latest commercial generation from Bosch, LRR4, is a monostatic multimodal radar that has six fixed antennas. The four central antennas can be properly fed to create a focused beam pattern with an opening angle of ±6 degrees (narrow FoV for detection range up to 250 m with a transmitted power up to 10 dBm) with minimal interference from traffic in adjacent lanes. In the near range, the LRR4's outer two antennas expand the FoV to ±20 degrees at a distance of up to five meters, to detect vehicles entering or leaving the vehicle's lane. Table 1 summarizes, with reference to recent vehicular radars proposed in the market, the performance and specifications of low-power automotive radar in terms of max distance, FoV at azimuth and elevation, accuracy (best case) achieved in terms of range, speed and angle, object separability and physical characteristics like size, weight and power consumption.

Radar Type	**Max. range**	**Azimuth FoV**	**Elevation FoV**	**Best accuracy (range, speed, angle)**	**Object separability (range, speed, angle)**	**Weight, Size, Power**
ARS408 Continental	250m	$\pm9^0$@250m $\pm45^0$@100m $\pm60^0$@20m	14^0@250m 20^0@20m	±0.1/0.4m near/far ±0.03 m/s $\pm0.1^0$	±0.1 m/s near, ±0.12 m/s far	330g, 13.8x9.1x3 cm^3 6.6W
LRR4-Bosch	250 m	$\pm6^0$@250m $\pm10^0$@100m $\pm15^0$@30m $\pm20^0$@5m	$\pm4.5^0$@200m	0.12 m 0.11 m/s $\pm0.3^0$	0.72 m 0.4 m/s $\pm4^0$ Max 24 targets	<240 g 7.8x8.1x6.2 cm^3 4.5 W
MRR-Bosch	160m	$\pm6^0$@160m $\pm10^0$@60m	$\pm 25^0$@36m $\pm42^0$@12m	0.12m 0.11 m/s ±0.3	0.72 m 0.66 m/s $\pm7^0$ Max 32 targets	<190g, 7x6x3cm^3 4.5W
MRRrear Bosch	80m	$\pm5^0$@70m $\pm75^0$@close (1 m)	none	0.12m 0.14 m/s $\pm0.8^0$		

Table 1: specifications of automotive radar, all at 76-77 GHz.

However, advanced digital radar signal processing, requiring nanoscale CMOS technology, is still implemented outside these radar-on-chip transceivers and only local raw data processing algorithms are implemented in the radar node, in a separate CPU. More complex radar data processing algorithms remain out-of-scope of current designs. With reference to the SAE classification in 6 assisted or autonomous driving levels from L0 to L5 discussed in Section I, the available automotive radar technology nodes are only suited for L3, i.e. assisted driving, where the human intervention is still needed. Moving to advanced autonomous solutions at L4 (vehicles are "designed to perform all safety-critical driving functions and monitor roadway conditions for an entire trip", although in some defined scenarios) or even L5 (full autonomous in every scenario) require much more complex signal processing capabilities, possibly exploiting machine learning techniques [40]. The challenges to face include:

- Radar image understanding and object tracking (obstacles, pedestrians, bikers, vehicles) [41] at very low missed detection/false-alarm rates.
- Radar data fusion with other mobility sensors.
- Low-latency reaction time, which implies real-time implementation of signal processing.
- Crowded environments with interference from radar sources of neighboring vehicles and V2I/V2V RF signals.
- Green radar to minimize the overall EM emissions of all radars mounted on-board all vehicles thanks to precise/adaptive beamforming, including waveform design, and/or passive radars [42].
- Correct identification/authentication of the proper radar trace and security against hacking or privacy violation.

III. Embedded signal processing toward cheap, low-power and real-time radar sensors

a. Radar SoC parameters

New opportunities to embed radar signal processing techniques in cheap, low-power and real-time SoC arise thanks to the technology evolution to pure CMOS, 45 nm or 28 nm nodes as in last single-chip radar released in [7-9]. For example, the SoC in [7] integrates for a cost less than 50 Euro and a power consumption of 2 W the entire mmWave RF and analog and digital baseband signal processing chain. It integrates two transmitters and four receivers, as well as two customer-programmable processors: a 600 MHz C674x DSP and a 200 MHz ARM® Cortex®-R4F microcontroller with 1.5 MB on-chip RAM. The on-chip memory is half devoted to radar data cube processing and half to cache memories for the two processors. The SoC allows for 12.5 dBm TX power and 14 (or 15) dB RX noise figure, with -95 (or -93) dBc/Hz phase noise at 1 MHz offset, in the 76 to 77 (or 77 to 81) GHz band. Being AECQ100 and ASIL-B qualified, operating in the -40 ^{0}C to 125 ^{0}C temperature range, the SoC in [7] is ready for automotive use. The computational capability of the SoC allows for 256-cells Constant False Alarm Rate Cell Averaging (CFAR-CA) implemented in 1.55 µs and 16-bit 256 (512) points Fast Fourier Transform (FFT) in 1.55 (3.61) µs. Thanks to the embedded DSP, the SoC implements MUSIC and ESPRIT technologies for high-resolution angle estimation. HW-based security accelerator are embedded like TRNG (True Random Number Generator), AES (Advanced Encryption Standard), and SHA2 (Secure Hash Algorithm) to address radar hacking and privacy violation issues. Fig. 2 reports an example of SoC radar architecture with such characteristics, considering for the RF part a heterodyne receiver with a high-speed ADC working at the intermediate frequency (IF) and a homodyne transmitter. It is worth noting that the Radar SoC architecture in Fig. 2 is just one possibility, since there are many different architectures from various chip

makers. The SoC radar in [7] can be configured for a detection unambiguous range of 80 m and maximum unambiguous speed of 90 km/h, with 35 cm distance resolution and 0.3 m/s velocity resolution. Such performance is achieved thanks to FMCW-based range-velocity estimation using 128 FMCW ramps x 4 channels x 256 points 3D FFT calculation, 425 MHz FMCW sweep bandwidth, 128 chirps (51 µs chirp duration and 7.5 µs reset time). The horizontal and vertical elevation FoV are 120^0 and 10^0 respectively. The same SoC can be reconfigured for a lower range of 20 m, but with higher resolution of 8.7 cm, by using a 1.725 GHz sweep bandwidth. Moving from CMOS 45 nm in [7] to 28 nm in [8] the memory and computational capability will double, thus enabling more complex radar algorithms to be implemented. Hereafter, we review the signal processing chain of the SoC of Table 2.

HW parameters (mmW front-end and baseband digital processing)								
Power	Cost	Tech.	RF, IF	TX power	RX NF	Phase noise	DSP	MCU
2.14W	<50 E	SoC 45nm	76-81 GHz, 5 MHz	12 dBm	15 dB	-95 dBc/Hz	600 MHz C674X	200 MHz ARM CortexRF4
Signal processing parameters (FMCW)								
Sweep Band B	Chirps P	Frame time	Tchirp/Treset	RX/TX channels	Detection	Angle-estimation	ADC	Range FFT
0.425 (1.725) GHz	128	7.5 ms	51/7.5 µs	4/2	CA-CFAR	MUSIC/ESPRIT	6.25 MSps	256
Radar system parameters								
Range	HFoV		VFoV		Max speed		Speed resolution	Range resolution
80 (20) m	120^0 (160^0 at 10 m)		10^0 (30^0 at 10 m)		90 (30) km/h		1 km/h	35 (8.7) cm

Table 2: HW and signal processing parameters of a SoC Radar with the architecture of Fig. 2

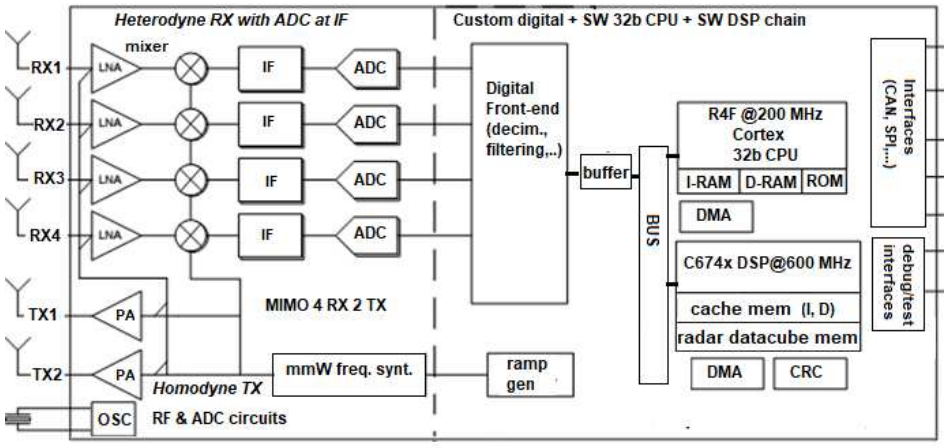

Fig. 2: Radar SoC architecture (76-81 GHz, FMCW, MIMO 4 RX/2TX).

b. Range and velocity estimation algorithm

All radars in Tables 1 and 2 operate in the 77 GHz band and adopt FMCW pulses to provide simultaneous range-velocity estimation in multi-target traffic scenarios. Continuous Wave (CW) radars are not able to provide measure of

the target distance, but only of their velocity. Thanks to the frequency modulation, FWCW radars are able to provide measures of both range and velocity. The estimation of target velocity can be done exploiting the Doppler effect. Being v_D the differential velocity between the vehicle of interest and the target (e.g. another car, a pedestrian, a biker, etc.) along the radar illumination direction, the reflected waves will be delayed by time $t_d=2(R\pm v_D t)/c$. The time-dependent delay causes a frequency shift in the received wave known as the Doppler shift $f_d=\pm 2v_D/\lambda$, which is inversely proportional to wavelength λ, and its sign is positive or negative, depending on whether the target is approaching or receding the radar [2]. The FMCW radar transmits periodic wideband FM pulses (chirps), whose frequency increases linearly during the pulse (see Fig. 3). A single FMCW pulse p(t) can be written as in Eq. (1):

$$p(t) = e^{i2\pi(fc+0.5Kt)t},\ 0<t<T_{chirp} \qquad (1)$$

where f_C, is the carrier frequency, T_{chirp} (51 μs in Table 2) is the chirp length, and $K=B/T_{chirp}$ is the sweep rate being B the sweep bandwidth (K=8.3 MHz/μs, B=425 MHz in Table 2). The signal received after reflection with a target is mixed (output of the receiver mixer in Fig. 2) with the transmitted signal to produce a low-frequency beat signal, whose frequency is linearly dependent on the range of the target. This operation is repeated for P consecutive pulses. Consecutive reflected pulses give a 2D waveform arranged across two time indices, where the slow time index p corresponds to pulse number while the fast time index n assumes that for each pulse. The corresponding continuous beat signal is sampled with frequency f_s to collect N samples within the duration time T (58.5 μs in Table 2). The latter includes the chirp time T_{chirp} and the rest time T_{res} (7.5 μs in Table 2). Fig. 3 represents the ideal case of $T_{res}=0$ and hence $T=T_{chirp}$. Assuming single target and neglecting reflected signal distortions, Eq. (2) shows the FMCW radar receiver signal x(n,p) as function of time indices n and p, where $\omega(n,p)$ is additive white Gaussian noise.

$$x(n,p) \sim \exp\left\{i2\pi\left[\left(\frac{2KR}{c}+f_d\right)\frac{n}{f_s}+f_d pT+\frac{2f_c R}{c}\right]\right\}+\omega(n,p) \qquad (2)$$

Discrete Fourier transform across fast time n can be applied to obtain the beat frequency f_b, which includes the information about both the target range (which is related to the time delay t_d in Fig. 3 between transmitted chirp and received signal) and the target velocity (which is related to the Doppler frequency shift f_d). Hence, applying a 2D FFT algorithm, a range-Doppler map can be produced [2]. In the range-Doppler map the peaks along the rows reveal the distance of a target, whereas the peaks along the columns reveal the speed of the target. To this aim, a peak detection algorithm has to be used. To identify valid targets in the presence of clutter, the threshold for the target detection should be properly chosen. If the amplitude of the spectrum at an estimated range is greater than some threshold, the target is

said to be detected. Thus, the threshold should depend on the noise or, in other words, on the clutter in the given system. As clutter increases, a higher threshold may be chosen. A simple Constant False Alarm Rate (CFAR) technique based on cell averaging (CA-CFAR) uses a sliding window to derive the local clutter level by averaging the multiple range bin samples. CA-CFAR is the technique used both in the SoC radar of Table 2 and by our single-board radar in [10]. To further increase the accuracy of detection other more sophisticated CFAR algorithms can be used, as the Ordered-Statistic (OS) or the Trimmed Mean (TM)-CFAR [2].

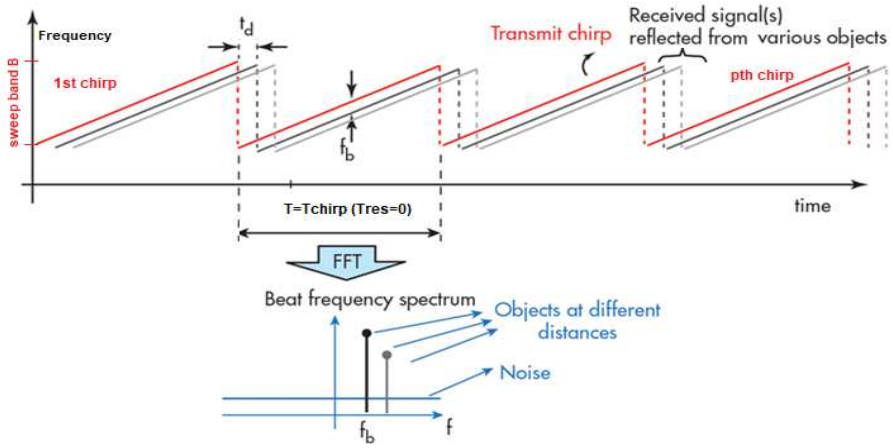

Fig. 3: FMCW range-velocity estimation, waveforms.

Moreover, to improve the performance, the CFAR algorithm could be followed by a binary integrator (e.g. with a M-out-of-N decision rule) as in Fig. 4, that shows the digital baseband signal processing chain implemented at University of Pisa for parking and road crossing surveillance in [10].

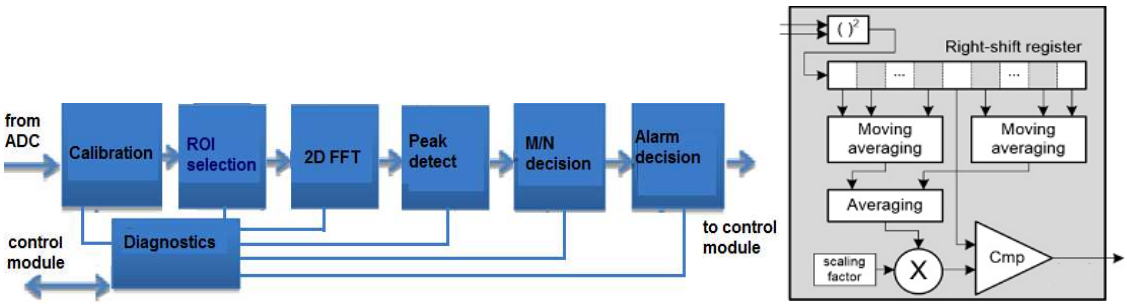

Fig. 4: Baseband digital signal processing architecture of a FMCW radar (left) for range-speed estimation and detail of CA-CFAR peak detection (right).

Fig. 5 shows an example of a range-Doppler map obtained with such FMCW radar. The range-Doppler image in Fig. 5 is obtained with 0 dBm (1 mW) transmitted power, P=256 FMCW ramps and 2048 samples/ramp, i.e. using a 256x2048 2D FFT, B=500 MHz sweep bandwidth, 12 bits ADC. Three different targets have been detected in this specific scene for a parking surveillance application: Target A at a distance of 81 m and with a relative speed of 21

km/h, Target B at a distance of 44 m and a relative speed of 5.5 km/h and Target C, almost still, at a distance of 77 m. The detected targets do not appear like a point in the range-Doppler map, but rather like an oval. This is due to the physical size of the targets but also to the resolution limits in distance and speed of the implemented FMCW radar sensor. Indeed, the limited sweep bandwidth B determines a limit on the distance resolution $dR = \frac{c}{2B}$, i.e. 30 cm at B=500 MHz. The speed resolution limit mainly depends on $\lambda/(2PT)$ and is 1 km/h at 77 GHz in the example case of λ= 4mm, P=128 and T=58 µs as in Table 2.

A convenient alternative to the chirp waveform is the double-chirp or triangular chirp, see Fig. 6. The positive slope of the signal indicates an up-chirp signal, while the negative slope a down-chirp signal with the same sweep bandwidth B. In the first interval T_{CPI} the up-chirp is transmitted, followed in the second T_{CPI} by a down-chirp.

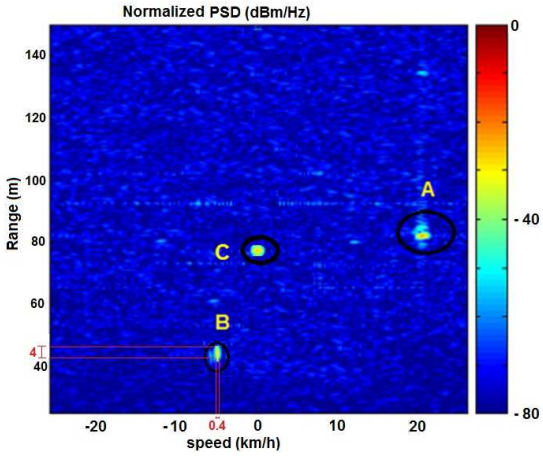

Fig. 5: Example of a range-Doppler map obtained with a FMCW radar sensor (256 chirps, 2048 sample/chirp, 0dBm TX, 500 MHz sweep bandwidth) with 3 targets.

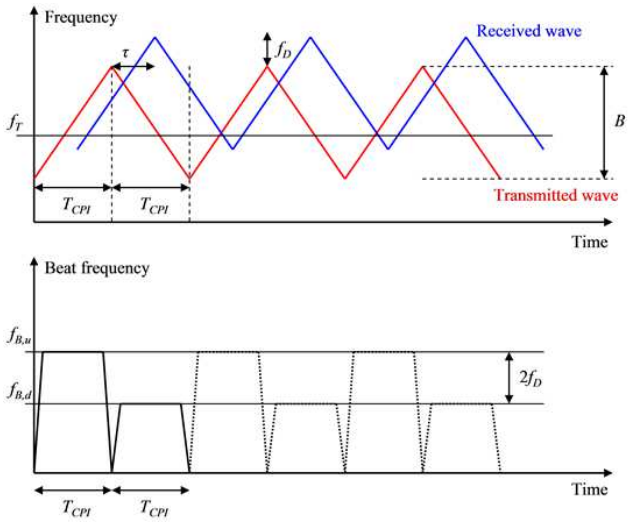

Fig. 6: Triangular chirp [3].

The advantage of this waveform compared to the single chirp is that in this case, for every triangular pulse, the radar has two beat frequencies $f_{B,u}$ and $f_{B,d}$, as shown in the bottom part of Fig. 6, both related to the range and Doppler frequency of the target. Then the radar can estimate at the same time both range and Doppler frequency [3]. It is worth noting that a triangular pulse provides unambiguous estimate of these target parameters only when a single target is present. In a multiple targets scenario, the triangular chirp provides an up and down beat frequency equation for each target, then for two targets 4 different ambiguous solutions. In this case alternative waveforms as stepped frequency (SF) CW, orthogonal frequency-division multiplexing (OFDM), and frequency shift keying (FSK) have been proposed as explained in [43].

c. Direction of arrival estimation

To implement direction of arrival (DOA) estimation, which is essential in the perception process, a multi-antenna receiver array is needed. In a realistic traffic scenario several targets are surrounding the radar that collects direct and multipath reflections from them. In such cases, to spatially resolve equidistant targets and deliver comprehensive representation of the traffic scene, angular location of targets should be estimated. In vehicular radars, the location of a target is often described in terms of a spherical coordinate system, which includes range, azimuth angle and elevation angle. The single antenna radar discussed before allows for range-velocity estimation but it lacks the information in terms of angular locations of the targets. The latter can be achieved by comparing the received signals of multiple receive channels placed at a pre-determined distance. Let's consider an antenna array located in plane X-Y, and let l be the abscissa corresponding to each receiver antenna position, e.g. 4 elements in the Uniform Linear Array (ULA) in Fig. 7, at distance d each (often in literature $d=\lambda/2$, and hence the total length of the ULA in Fig.7 would be $L=2\lambda$). Let (R_q, θ_q) be the position of the qth target in spherical coordinates, moving with relative velocity v_q to the radar. With the help of far field approximation for the qth target, the round-trip time delay between a transmitter located at the origin and the receiver positioned at coordinate l is given by $\tau_{lq} = \frac{2(R_q+v_q t)+ldsin(\theta_q)}{c}$. Hence, a 3D FMCW radar signal can be obtained, that in case of Q targets can be expressed as in Eq. (3), where α_q is a complex scalar whose magnitude represents for the qth target the attenuation due to antenna gain, path loss, and the RCS (Radar Cross Section) of the target. The delay term τ_{lq} creates uniform phase progression across antenna elements, which permits the estimation of the angle by FFT in spatial domain. Thus, 2-D location (range and angle) and speed of targets can be jointly estimated

by 3-D FFT. The relevant cube of data of range, FMCW ramps and multiple receiving channels is shown in Fig. 7 (right).

$$x(l,n,p) \sim \sum_{q=0}^{Q-1} \alpha_q \exp\left\{ i2\pi \left[\left(\frac{2KR_q}{c} + f_{dq} \right) \frac{n}{f_s} + \frac{f_c l d \sin(\theta_q)}{c} + f_{dq} pT + \frac{2f_c R_q}{c} \right] \right\} + \omega(l.n,p) \quad (3)$$

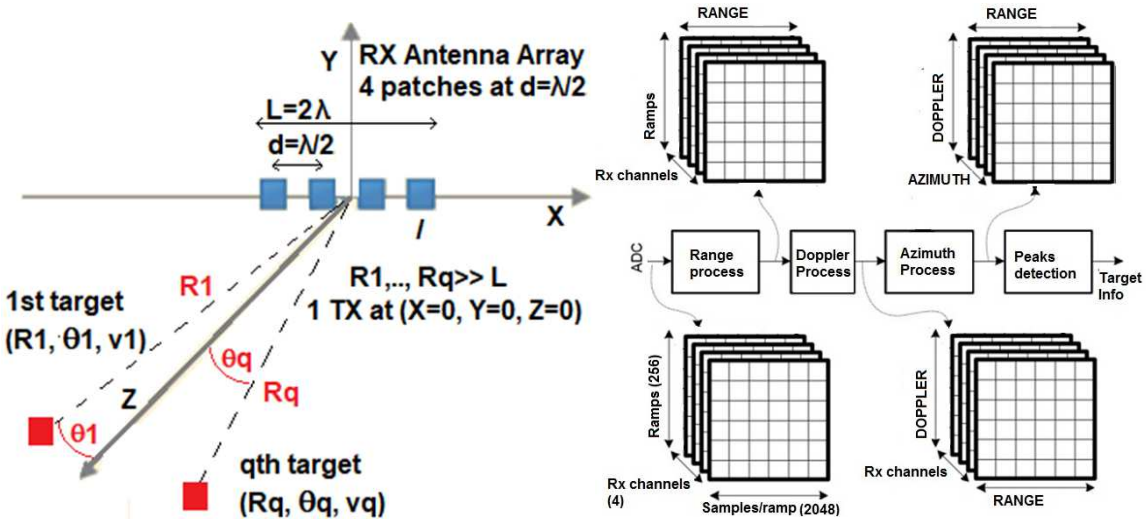

Fig. 7: Range-velocity-angle estimation with 3D FFT thanks to a multi channel receiver array (left), e.g. ULA with 4 channels at d=λ/2, and corresponding radar data cube (right).

It is worth noting that the FMCW 3D-FFT radar with CA-CFAR peak detection we have proposed has been implemented at University of Pisa at board level with separate chips for mmW transceivers, analog front-end and ADC and baseband digital signal processing (while that in Table 2 is integrated at single chip level). The digital signal processing is implemented in a Zynq XA7Z020 device. It is a pure digital FPSoC integrating Dual-Core ARM 32b Cortex-A9 Based Application Processor Unit, with 2.5 DMIPS/MHz computational capability, clocked at 200 MHz, plus NEON hardware instruction set extension (128-bit, single-instruction multiple-data architecture), plus FPGA resources plus a large set of peripherals. The peripherals include external SDRAM, non-volatile memory controllers, 2 CAN interfaces, 1 Mbyte of on-chip RAM memory. The 3D-FFT FMCW computing unit occupies roughly 94% of available Zynq XA7Z020 resources in terms of Flip-Flops, memory blocks and DSP blocks (mainly with multiply&add capabilities) and 46% of available Look-up Tables for custom combinatorial logic.

d. Adaptive beamwidth

It is worth noting that differently from what has been analyzed in survey papers [2], rather than a fixed specification for the beamforming, the last generation of vehicular radars in Tables 1 and 2 supports multiple antennas and adaptive beamforming. As an example, in Table 1 the azimuth FoV in long range radars is adapted from a minimum of $\pm 9^0$ to a

maximum of $\pm 60^0$ when the range varies from 250 m to 20 m, whereas in medium range radars is adapted from a minimum of $\pm 5^0$ to a maximum of $\pm 75^0$ when the range varies from 70 m to 1 m. Often, in commercial devices the adaptive beamformer is obtained by a proper mix of the antennas in the array. For example, in the above mentioned LRR4 sensor from Bosch, 4 central antennas are properly fed to create a focused beam pattern with an azimuth FOV of ±6 degrees at maximum distance of 250 m, whereas 2 outer antennas are used to achieve an extended FoV of ±20 degrees at a target distance below 5 m.

It is worth noting that a narrowband beamforming array usually characterizes mmWave automotive radars. Indeed, the fractional bandwidth of mmW radar signals is within 5% (e.g. 1 to 4 GHz bandwidth at about 80 GHz in Tables 1 and 2). Moreover, the time delay τ_{max} between the first and last elements of the antenna array is usually so small that the signals received by the opposite ends of the array are still correlated with each other. Indeed, in the example case of an ULA of M elements, with $\lambda/2$ spacing, $\tau_{max} = \frac{(M-1)\cdot\lambda}{2C}$, which corresponds to a delay in the range 10^{-11} to 10^{-10} ps when considering the typical parameters of on-chip/in-package radars in Tables 1 and 2.

A special note has to be done on the elevation antenna FoV. Thanks to it, the radar sensing system may achieve a wide opening angle at close range, so a pedestrian stepping out into the road from behind a parked car, is detected at an early stage. An independent mode for height measurement using an elevation antenna enables the system to classify reliably objects and to brake safely, even when the object is stationary.

When designing an antenna for on-chip/in-package radar applications (whose detailed discussion is out of the scope of this paper) achieving a wide FOV is often a contrasting requirement vs. other key performance parameters such as high gain and compact size. One option to achieve the required azimuth and elevation FoV is exploiting an antenna array by placing the antennas so that the operation in MIMO mode (see further discussion in Section IV.b) synthesizes a 2-D virtual array, thus enabling angle estimation along both azimuth and elevation. Such technique is already exploited by the latest commercial generation of mmW radar sensors from Texas Instruments (TI) [44] for automotive and industrial applications. For example, the Radar-on-chip sensor in Table 2 sustains 2 TX and 4 RX antennas; other state-of-art devices [44] with the same architecture support 3 TX and 4 RX antennas. As detailed in Section IV.b Fig. 8, if the 2 (or 3) TX antennas and the 4 RX antennas are placed on the same azimuth plane (i.e. at the same height) a virtual array of 8 (or 12) RX antennas is obtained on the azimuth plane. Instead, if the antennas are placed so that one

or more antennas are at a different height vs. the other elements then a virtual array also along the elevation is obtained, see Fig. 9 in Section IV.b for more details.

e. Waveform design

The adaptability and selection of the radar waveform is a key issue in embedded automotive radar since this affects the performance in terms of range resolution, velocity resolution, angular direction, SNR, the probability of target detection, and, in the case of FMCW radars, number of targets that can be resolved without ambiguity (ghost targets) [43]. In general, the radar waveforms can be characterized whether or not they are CW, pulsed and frequency, or phase modulated. Modulated radar waveforms include for example FMCW, stepped frequency continuous wave (SFCW), orthogonal frequency-division multiplexing (OFDM), and frequency shift keying (FSK). Each waveform type has a certain advantage in processing, implementation, and performance as proposed in Table 3. The most common, in vehicular radars, are the linear frequency modulated CW (chirps). In unmodulated CW radar, a conjugate mixing of a high-frequency transmitted and received signal produces the output signal at the Doppler frequency of the target. The resolution of frequency measurement is inversely proportional to the time duration of the signal capture. The continuous nature of the waveform precludes round-trip delay measurement, which is necessary for range estimation of the target. As discussed above, FMCW, also known as linear frequency modulation (LFM) or chirp, is used for simultaneous range and velocity estimation. The range resolution is inversely proportional to the bandwidth of the FMCW signal and is independent of pulsewidth. For example, short-range FMCW radars use UWB waveforms to measure small distances with higher resolution. The Doppler resolution is a function of pulsewidth and the number of pulses used for the estimation.

In contrast to FMCW waveforms, the frequency of FSK and SFCW varies in a discrete manner [2]. In this case, the range profile of the target and the data collected at discrete frequencies form the inverse Fourier transform relationship. Also, hybrid waveform types can be employed to achieve additive performance. FSK waveform can be combined with multislope FMCW waveform to overcome ghost targets in radar processing [14]. Similarly, alternate pulses of CW and FMCW are used to accurately estimate range and Doppler [9].

OFDM can be viewed as another multifrequency waveform that offers unique features of the joint implementation of automotive radar and vehicle-to-vehicle communications [11, 12]. For the radar operation, the orthogonality between OFDM subcarriers is ensured by choosing carrier spacing more than maximum Doppler shift, and the cyclic prefix

duration is selected greater than the longest round-trip delay. The range profile is estimated through frequency domain channel estimation.

Waveform	TX signal	Detection by	Range, Doppler resolution	note
Pulsed CW	$rect\left(t/T_p\right)\cdot e^{i2\pi f_c t}$	Correlation	$\Delta R = c\frac{T_p}{2}, \Delta f_d = \frac{1}{T_p}$	ΔR depends on 1/ Δf_d
FMCW	$e^{i2\pi(f_c+Kt)t}, K = B/2T$	Conjugate mix	$\Delta R = \frac{c}{2B}, \Delta f_d = \frac{1}{PT}$	*P*=number of ramps each with duration *T*
SFCW	$e^{i2\pi f_n t}, f_n = f_c + (n-1)\Delta f$	IFFT (inverse FFT)	$\Delta R = \frac{c}{2B}, \Delta f_d = \frac{1}{PT}$	$\Delta f\ sets\ Rmax$, *P*=number of ramps each with duration *T*
OFDM	$\sum_{n=0}^{N-1} I(n)\cdot e^{i2\pi(f_c+n\Delta f)t}$	Channel estimation in freq. domain	$\Delta R = \frac{c}{N\Delta f}, \Delta f_d = \frac{1}{PT_N}$	N=number of carriers, *P*=number of OFDM blocks of duration T_N I(t) is an arbitrary sequence

Table 3: Main waveforms that can be selected in single-chip CW radar

IV. Advanced radar signal processing

a. Embedded HPC for high-end signal processing

Sect. III has discussed the scenario to achieve a low-cost, low-power and small size radar sensors to be mounted on-board a vehicle (multiple sensors covering short/medium range and medium/long range and positioned in different places to achieve a 360^0 coverage). From a signal processing point of view, a multi-antenna FMCW-based technique for range-speed-angle estimation, with adaptive beamforming and diverse waveform selection has been discussed and single chip and single board implementations have bene reviewed. This scenario does not consider the issues arising in case all vehicles are equipped with multiple remote sensors, and are interconnected with V2V/V2I technologies and hence issues of spectrum occupation and interference will arise. This is why advanced signal processing techniques may be needed and are discussed below: MIMO radar to further improve resolution and cognitive radar to achieve a full adaptability to the environment. While the signal processing capability integrated in the SoC radar of Fig. 2 is on the order of few GOPS (Giga Operations Per Second), emerging automotive HPC processors are promising to increase this value by one order of magnitude at least. For example, the recently (March 2018) launched Renesas-H3 integrates in 16 nm technology a PowerVR GX6650 GPU with 192 ALU cores for 3D Graphics (more than 100 GOPS) plus 8 64-bit ARM cores (4 Cortex-A57 and 4-Cortx-A53) and 1 32–bit Cortex-R7 (main controller) offering extra 40 GOPS. Announced new embedded HPC designs from INTEL and NVIDIA are further increasing these numbers. EyeQ5 SoC from MobilEye (now INTEL) is targeting 24000 GOPS at 10 W. Xavier AI car's computer from NVIDIA is targeting 30000 GOPS with a power consumption of 30 W (thanks to 8 ARM 64-bit cores plus a 512-core Volta GPU, a Video

Processing Unit supporting 8K video decode and encode and High Dynamic Range, as well as a computer vision accelerator).

b. MIMO radar

MIMO radar systems employ multiple transmitters, multiple receivers, and multiple waveforms. MIMO radars can be classified as widely separated or co-located. In widely separated MIMO radar, transmit-receive antennas capture different aspects of the RCS of a target, while in colocated MIMO radar, the RCS observed by each antenna element is indistinguishable. Due to compact size requirements, automotive radar typically exploits colocated MIMO radars, which are compact in size. For proper transmitter spacing, the colocated MIMO radar can emulate a larger aperture phased array radar, i.e. a virtual array. For the MIMO radar processing, let's consider L_T and L_R a number of transmit and receive antenna elements, respectively (L_T=2 and L_R=4 for the SoC Radar in Fig. 2, and for the example in Fig. 8). Suppose that d_T and d_R represent the corresponding transmit (yellow dots in Fig. 8) and receive (blue dots in Fig. 8) antenna spacings. Also, assume that transmit and receive antenna positions in Cartesian coordinates are given by l_T and l_R. Hence, the 2-D FMCW mixer output signal across fast time and aperture is given by Eq. (4). If $d_T = L_R\, d_R$ then MIMO radar imitates a regular 1-D array radar with single transmit and $L_R \cdot L_T$ receive antenna elements (virtual array representation [2]). Hence, the spatial resolution of FFT-based target imaging can be improved by the factor of L_T.

$$x(l_T, l_R, n) \sim \sum_{q=0}^{Q-1} \alpha_q \exp\left\{ i2\pi \left[\frac{2KR_q}{c}\frac{n}{f_s} + \frac{f_c(l_T d_T + l_R d_R)\sin(\theta_q)}{c} + \frac{2f_c R_q}{c} \right] \right\} + \omega(l_T, l_R, n) \quad (4)$$

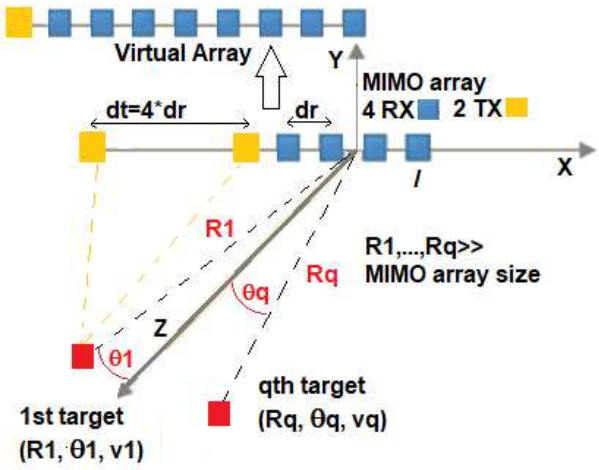

Fig. 8: Co-located MIMO radar with 2 TX and 4 RX antenna elements. 1-D virtual array.

As already discussed in Section III. D of this survey, the TX and RX antenna elements can be also placed so that the operation in MIMO mode synthesizes a 2-D virtual array, see example in Fig. 9, instead of the 1-D virtual array as in

Fig. 8. For example, the commercial TI AWR1443 and IWR1443 radar sensors in [44] for automotive and industrial uses, exploit the 2D array configuration in Fig. 9.d to reach an elevation FOV of 30 degrees.

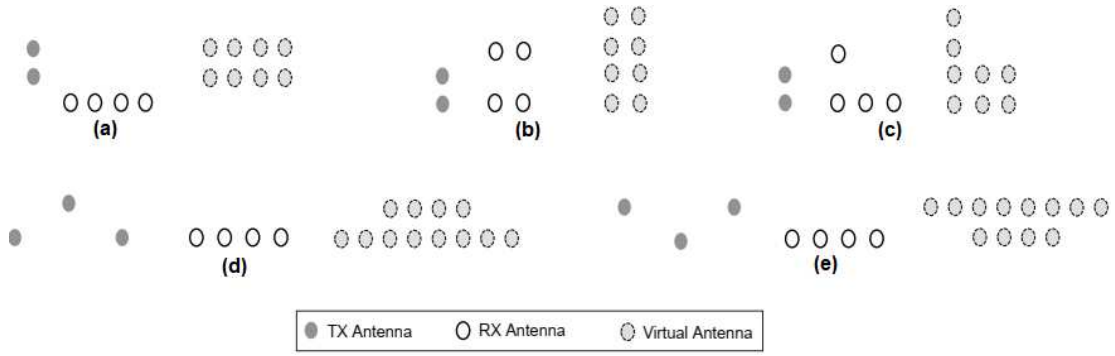

Fig. 9: 2-D virtual antenna array using 2 TX/4 RX elements in (a), (b), (c), 3 TX/4 RX elements in cases (d), (e)

One of the challenging aspect of MIMO radar is the selection of waveforms. The waveforms can be made orthogonal in the frequency, time, or code domain. Consequently, the matched filter design at the receiver varies, which is necessary to separate the reflected waveforms originating from different transmitters. From the basic FMCW radar signal given in Section III, various orthogonal waveforms can be constructed as reported in Table 4. More details on vehicular MIMO radars are provided in the paper [15] in this special issue.

Type	Pulse expression	Notes
Beat frequency division	$\exp\left\{i2\pi\left[(fc-\Delta f_b)t+0.5Kt^2+0.5\left(\frac{\Delta f_b^2}{K}\right)\right]\right\}$	Δf_b is the frequency offset introduced for waveforms orthogonalization. The last term in the exponential corresponds to residual video phase compensation, which is necessary for coherent receiver processing
Modulation constant division	$\exp\{i2\pi[fc+0.5(K+\Delta K)t]t\}$	The modulation constant or chirp rate offset is given by ΔK, which is obtained by varying the pulse period. The bandwidth at each transmitter remains the same to maintain the range resolution. The reset time between the pulses ensures the synchronization at the receiver.
Code division	$\exp\{i2\pi[fc+0.5Kt]t+0.5\beta(t)\}$	$\beta(t)$ corresponds to the binary phase-shift keying (BPSK) signal with a low update rate that assumes values ±1 . The bandwidth of the BPSK signal is kept smaller to ensure proper operation of the FMCW radar

Table 4: MIMO radar waveform design

c. Cognitive radars

One fundamental reality for automotive radars is the problem of mutual interference due to multiple radars operating closely and simultaneously and that of interference with communication systems working in the same mmW bandwidth, particularly when 5G systems will be fully operating. A detailed analysis of these interferences is provided in [45]. This issue of spectrum crowding can be partially addressed by traditional modes of operation, such as spatial

signal processing and beamforming [46]. But, more likely, future automotive radar systems must be able to anticipate the behavior of other emitters in the operational environment and to adapt their transmissions in a cognitive fashion based upon the spectrum availability. As cognitive radio systems devoted to communications, cognitive radar systems should then perform the spectrum sensing function, which has the goal to obtain necessary observations about the radio frequency channel, such as the presence of other users and the appearance of spectrum opportunities (free channels) where it is possible to transmit without interfering. Spectrum sensing can be performed via two different architectures: single-radio and dual-radio. In the single-radio architecture, only a specific time slot of the signal at the radar receiver is allocated for spectrum sensing. In dual-radio sensing architecture, one radio chain is dedicated to the radar operations while the other chain is dedicated to spectrum sensing. Note that a single antenna would be sufficient for both chains [13] and would make it easy to realize the cognitive system in a SoC. As detailed in [46], there are multiple techniques to perform the spectrum sensing, as already implemented in cognitive radios. The open literature mainly focuses on energy detector (ED), feature detector (FD), and matched filter (MF) detector techniques. In general, based on the knowledge acquired by analyzing the environment through the sensing block, the automotive radar should be able to change on-the-fly its carrier (for OFDM radars), transmit sub-band, chirp slope or waveform shape, code, Pulse Repetition Interval (PRI), etc. in order not only to reduce the cross-interference between coexisting radars and/or communication systems, but also to improve the range and frequency resolution and the signal-to-noise ratio. Thus, the cognition is not limited only to the reduction of the interference, but can be beneficial as well for the radar detection and tracking performance, as shown for instance in [47] and [48].

d. Passive radars

To mitigate the spectrum crowding problem at mmW bands, another advanced radar signal processing technique to be exploited in the future is the use of passive radars [49, 50]. They are bistatic radars that make use of emissions from a non-cooperative transmitter of opportunity, such as broadcast, communications, or radio-navigation transmitters rather than a dedicated, co-operative radar transmitter. In large ground-based radars, emissions from FM radio stations, Digital Audio Broadcasting and Digital Video Broadcasting, 3G and 4G cellular signals are used for target detections purposes. While in active radar sensors, the time of transmission and the transmitted waveform are exactly known, and this allows the target range, speed and DoA to be estimated, even with embedded systems, as discussed in previous sections, a passive radar is missing such information directly. To overcome this issue, a dedicated receiver channel

acting as a reference channel can be used to monitor each non-cooperative transmitter being exploited, and dynamically sample the transmitted waveform. Differently from active radars, the detection range in passive radars is also a function of the deployment geometry, as the distance of the passive receiver from the non-cooperative transmitter determines the level of external noise against which the targets must be detected. In addition, passive radar accuracy is a strong function of the deployment geometry and the number of receivers and transmitters being used.

Differently from other applications, such as early warning, harbor protection, etc., where the research has already produced many prototypes, for automotive applications, the passive radar technology is still seen as immature, and the reliance on third-party illuminators and the complexity of deployment are in contrast with the need of high functional safety level of autonomous driving.

A promising evolution of the passive radar concept, exploiting also the deployment of the emerging 5G technology, for automotive use has been recently presented in [49]. These works introduce the principle of cooperative passive coherent location (CPCL), which is seen as an integrated radar service of future mobile radio networks, such as 5G. Whereas passive radar technology does not consider any cooperation between radar illuminators and radar sensors, the CPCL concept assumes that all radar nodes belong to the same network. This way, CPCL will turn the mobile radio networks into a distributed MIMO radar network, which opens a wide scope of cooperation between sensor nodes including cooperative bi-/multi-static target scene illumination, radar data networking, and radar sensor fusion. Such technology is applicable to several applications involving networking nodes, such as intelligent transport systems and logistics. Besides 5G, also V2V and V2I links may be used to sustain the CPCL concept.

V. Conclusions and evolution trends

Radars-on-Chips/in-Package have seen a huge development over the last 20 years, since 1999 when Mercedes mounted the first commercial vehicular radar on its top class cars. Thanks to the technology improvements in SoCs and SiPs, in embedded high performance computing and to new investments, the radar is becoming more and more an ubiquitous sensor, available with low cost and low-power in a large volume market. When it appeared for the first time on the market, the radar on chip was able to perform very simple signal processing, with a single antenna and at high cost. Nowadays, the modern radar systems are able to perform much more complex signal processing algorithms, with multiple antennas and orthogonal waveforms as in the MIMO radars, with increased range and frequency resolutions, and can be connected in network with other radars and other sensors for safer driving or intelligent transportation

systems. Moreover, the evolution has not reached yet a steady-state. It is easy to foresee that in the future new on-chip radars will be cognitive, able to adapt their bandwidth and transmit waveforms based on the environment and the target features, then less sensitive to interferences and with improved detection and tracking capabilities. To mitigate the spectrum crowding problem at mmW bands, another option to be exploited in the future is the use of passive radars. By making use of emissions from a non-cooperative transmitter of opportunity, this technology promises to be green, reducing power consumption and EM interference emission. Although it is still not mature, and its reliance on third-party illuminators and on the scene deployment are in contrast with the need of autonomous driving for high functional safety levels in every condition, new sources of opportunity will come from 5G communications systems, as well as the V2V and V2I signals. To this aim, new sensing schemes are emerging, where multiple passive MIMO radar nodes can cooperate to create a reliable and ubiquitous radar service that may be adaptive, reconfigurable, and cognitive.

References

[1] A. Mukhtar, et al., “Vehicle detection techniques for collision avoidance systems: a review”, IEEE Trans. on Intelligent Transportation Systems, vol. 16, n. 5, pp. 2318-2338, 2015

[2] S. Patole, et al., “Automotive radars: A review of signal processing techniques”, IEEE Signal Proc. Magazine, vol. 34, n.2, 2017, pp. 22-35

[3] S. Saponara, E. Ragonese, M. Greco, B. Neri, G. Palmisano, Highly integrated low-power radars, Artech, House, 2014

[4] R. Hult, R. Campos, E. Steinmetz, L. Hammarstrand, P. Falcone, H. Wymeersch, “Coordination of cooperative autonomous vehicles: toward safer and more efficient road transportation”, IEEE Signal Processing Mag., vol. 34, n. 1, pp.74-84, 2017

[5] F. Pieri, C. Zambelli, A. Nannini, P. Olivo, S. Saponara, “Consumer electronics is redesigning our cars? Challenges of integrated technologies for sensing, computing and storage”, IEEE Consumer Electronics Magazine, vol. 7, n. 4, 2018

[6] I. Gresham, N. Jain, T. Budka, A. Alexanian, N. Kinayman, B. Ziegner, S. Brown, P. Staecker, "A compact manufacturable 76–77 GHz radar module for commercial ACC applications", IEEE Trans. Microwave Theory Tech., vol. 49, n. 1, pp. 44-58, 2001.

[7] J. Singh, B. Ginsburg, S. Rao, K. Ramasubramanian, “AWR1642 mmWave sensor: 76–81-GHz radar-on-chip for short-range radar applications”, Texas Instruments doc. N. SPYY006, 2017

[8] D. Guermandi, et al., “A 79-GHz 2x2 MIMO PMCW Radar SoC in 28-nm CMOS,” IEEE Journal Solid-State Circuits, vol. 52, n. 10, pp.2613-2626, Oct. 2017.

[9] K. Ramasubramanian, B. Ginsburg, “AWR1243 sensor: Highly integrated 76–81-GHz radar front-end for emerging ADAS applications”, Texas Instruments doc. N. SPYY003, 2017

[10] S. Saponara, B. Neri, “Radar Sensor signal acquisition and multidimensional FFT processing for surveillance applications in transport systems”, IEEE Trans. on Instrumentation and Measurement, vol. 66, n. 4, pp. 604-615, 2017

[11] A.A. Lopez et al. “Coherent Signal Processing for Traffic Flow Measuring Radar Sensor”, IEEE Sensor Journal, vol. 18, n. 12, pp. 4803-4813, 2018

[12] F. Engels, P. Heidenreich, A. M. Zoubir, F. K. Jondral, M. Wintermantel, “Advances in Automotive Radar A framework on computationally efficient high-resolution frequency estimation”, IEEE Signal Processing Magazine, March 2017, pp. 36-46

[13] M.Greco, F.Gini, P.Stinco, K. Bell, "Cognitive Radars: On the Road to Reality: Progress Thus Far and Possibilities for the Future", IEEE Signal Processing Magazine, Vol. 35, No.4, pp.112-125, July 2018.

[14] Special Issue on Machine Learning for Cognition in Radio Communications and Radar, IEEE Journal of Selected Topics in Signal Processing, vol. 12, n. 1, Feb. 2018

[15] S. Sun, A. Petropulu, H.V. Poor, H. Vincent, "MIMO Radar for ADAS and Autonomous Driving: Advantages and Challenges", IEEE Signal Processing Magazine, Special issue on Advances in Radar Systems for Modern Civilian and Commercial Applications, 2019.
[16] G. Hakobyan, "High-Performance Automotive Radar: A review of Signal Processing Algorithms and Modulation Schemes", IEEE Signal Processing Magazine, Special issue on Advances in Radar Systems for Modern Civilian and Commercial Applications, 2019
[17] Yu Li et al., "Optimal extrinsic calibration between a stereoscopic system and a Lidar", IEEE Transactions on Instrumentation and Measurement, vol. 62, n. 8, pp. 2258-2269, 2013
[18] Velodyne Lidar HDL32, "High-definition real-time 3D LIDAR", doc. 97-0038 rev. F, pp.1-2, 2016
[19] Zhiwei Xiong, Yueyi Zhang, Feng Wu, Wenjun Zeng, "Computational Depth Sensing: Toward high-performance commodity depth cameras", IEEE Signal processing Magazine, vol. 34, n. 3, pp. 55-68, 2017
[20] Yibo Zhu, "60 GHz mobile imaging radar", ACM HotMobile'15, 2015, Santa Fe, USA, pp. 65-80
[21] E. Piuzzi, "Complex Radar Cross Section measurements of the human body for breath-activity monitoring applications", IEEE Trans. on Instrumentation and Measurement, vol. 64, n. 8, pp. 2247 – 2258, 2015
[22] T. Huang et al., "FMCW based MIMO imaging radar for maritime navigation", Progress in Electromag. Research, vol. 115, 327-342, 2011
[23] Sirio-OD Automatic Detection of Obstacles on the Track.
Available at: http://www.starsrailway.com/download/Brochure_Sirio_OD.pdf
[24] W. Wang et al, "Design and implementation of a FPGA and DSP Based MIMO Radar imaging system", Applications of Wireless Communications, pp. 518-526, 2015.
[25] S. Scherr, "An efficient frequency and phase estimation algorithm with CRB performance for FMCW radar applications", IEEE Trans. on Instrumentation and Measurement, vol. 64, n.7, pp. 1868–1875, 2015
[26] J. Hasch et al., "Millimeter-wave technology for automotive radar sensors in the 77 GHz frequency band", IEEE Trans. on Microwave theory and technique, vol. 60, n. 3, pp. 845-860, 2012.
[27] C. Baer, "Contactless detection of state parameter fluctuations of gaseous media based on an mm-wave FMCW radar", IEEE Trans. on Instrumentation and Measurement, vol. 64, n. 4, pp. 865 – 872, 2015.
[28] G. Rubio-Cidre et al., "DDS-Based signal-generation architecture comparison for an imaging radar at 300 GHz", IEEE Trans. on Instrumentation and Measurement, vol. 64, n. 11, pp. 3085 – 3098, 2015.
[29] Sangdong Kim, Daegun Oh, and Jonghun Lee, Member, IEEE, Joint DFT-ESPRIT Estimation for TOA and DOA in Vehicle FMCW Radars, IEEE Antennas and Wireless Propagation Letters, vol. 14, 2015.
[30] A. Laribi, A new height-estimation method using FMCW radar Doppler beam sharpening, EUSIPCO 2018
[31] P. Kumari et al., IEEE 802.11ad-based Radar: An Approach to Joint Vehicular Communication-Radar System, 2018, IEEE Trans. on Vehicular Technology, vol. 67, n.4, 2018.
[32] M. Mehrnoush, "Coexistence of WLAN Network with Radar: Detection and Interference Mitigation, IEEE Trans. on Cognitive Communications and Networking, 3 (4), 2017.
[33] P. Papadimitratos, A. La Fortelle, K. Evenssen, R. Brignolo, S. Cosenza, "Vehicular communication systems: Enabling technologies applications and future outlook on intelligent transportation", IEEE Communication Magazine, vol. 47, n. 11, pp. 84-95, 2009.
[34] S. Lutz, K. Baur, T. Walter, "77 GHz lens-based multistatic MIMO radar with colocated antennas for automotive applications", IEEE Microwave Symp. Dig., pp. 1-3, 2012.
[35] J. D Wit, W. Van Rossum, A. D Jong, "Orthogonal waveforms for FMCW MIMO radar", IEEE Radar Conf., pp. 686-691, 2011.
[36] F. Engels, et al. "Automotive MIMO radar angle estimation in the presence of multipath", IEEE Radar Conference 2017
[37] I. Bilik, "Automotive MIMO Radar for Urban Environments", IEEE Radar Conference 2016
[38] C. Vasanelli, R Batra, C. Waldschmidt, "Optimization of a MIMO Radar Antenna System for Automotive Applications", IEEE EUCAP 2017, pp. 1113-1117
[39] S. Lutz, et al., "Lens-based 77 GHZ MIMO radar for angular estimation in multitarget environments," International Journal of Microwave and Wireless Technologies, 2014, 6(3/4), 397–404.
[40] W. Li, S. Fortunati, M.S. Greco, F. Gini, "Waveform optimization for multi-target detection with a reinforcement learning approach", *Asilomar 2018,* US, October 2018
[41] D. M. Gavrila, "Sensor-based pedestrian protection", IEEE Intell. Syst., vol. 16, no. 6, pp. 77-81, 2001.
[42] P. Samczynski et al., "A Concept of GSM-based Passive Radar for Vehicle Traffic Monitoring, Microwaves", Radar and Remote Sensing Symposium, 2011, Kiev, Ukraine, pp. 271-274

[43] H. Rohling, M. Kronauge, "Continuos waveforms for automotive radar systems", ch. 7 in Waveform Design and Diversity for Advanced Radar Systems, Edited by F. Gini, A. De Maio and L. Patton, IET Radar, Sonar and Navigation Series 22, 2012.
[44] S. Rao, A. Ahmad, J. C. Roh, S. Bharadwa "77GHz single chip radar sensor enables automotive body and chassis applications", TI application note SPRY315, Dec 2017, pp.1-11
[45] S. Alland, W. Stark, M. Ali, M. Hegde, "Interference in Automotive Radar Systems", IEEE Signal Processing Magazine, Special issue on Advances in Radar Systems for Modern Civilian and Commercial Applications, 2019.
[46] J Lunden; V. Koivunen; H. V. Poor, "Spectrum Exploration and Exploitation for Cognitive Radio: Recent Advances ", IEEE Signal Processing Magazine, 2015, Vol. 32, No. 3, pp. 123 – 140.
[47] G. E. Smith, Z. Cammenga, A. Mitchell, K. L. Bell, J. T. Johnson, M. Rangaswamy, and C. J. Baker, "Experiments with cognitive radar," IEEE Aerospace and Electronics Systems Magazine, special issue on Waveform Diversity: Part II, vol. 31, no. 12, pp. 34-46, Dec. 2016.
[48] S. Haykin, Y. Hue, P. Setoodeh, "Cognitive Radar: Step toward Bridging the Gap Between Neuroscience and Engineering", Proceedings of the IEEE, vol. 100, no. 11, pp. 3102-3130, 2012.
[49] R. S. Thoma, C. Andrich, G. Del Galdo, M. Dobereiner, M. A. Hein, M. Kaske, G. Schafer, S. Schieler, C. Schneider, A. Schwind, P. Wendland, "Coperative passive coherent location: a promising 5G service to support road safety", arxiv 1802.04041, Dec 2018, available at https://arxiv.org/pdf/1802.04041
[50] L. Zheng and X. Wang, "Super-resolution delay-doppler estimation for ofdm passive radar," IEEE Transactions on Signal Processing, vol. 65, n. 9, pp. 2197–2210, May 2017

Authors' Biography:

Sergio Saponara, (SM'12), sergio.saponara@unipi.it, is Full Professor of Electronics at University of Pisa and CTO and co-founder of IngeniArs srl. He co-authored more than 300 scientific publications and 18 patents. He was Marie Curie Research Fellow at IMEC (Belgium). He is IEEE DL and co-founder of the SiG IoT of IEEE CAS and SP societies. He is AE of many IEEE, IET, SpringerNature and MDPI journals. He contributed to organizing committees of about 150 IEEE and SPIE conferences. He is responsible of the summer school "Enabling Technologies for IoT" and CrossLab "Industrial IoT" and of many National, EU and Industrial funded projects.

Maria Sabrina Greco, (F'11), maria.greco@unipi.it, is Full Professor at the Dept. of Information Engineering, Pisa University. She's co-recipient of the 2001 and 2012 IEEE AES Society's Barry Carlton Awards for Best Paper and recipient of the IEEE AESS 2008 Fred Nathanson Young Engineer of the Year award. She has been general-chair, technical program chair and organizing committee member of many international conferences. She's Associate Editor of IET Proceedings – RSN, of the Springer *Journal of Advances in Signal Processing*, Senior Area Editor of IEEE TSP and VP Publications of IEEE AESS. Her general interests are in the areas of statistical signal processing, estimation and detection theory.

Fulvio Gini, (F'06), fulvio.gini@unipi.it, received his Dr.-Ing. and Ph.D. degrees in electronic engineering from the University of Pisa, Italy, in 1990 and 1995, respectively. Currently, he is a full professor in the Department of Information Engineering at the University of Pisa. He has received several awards, including the 2001 and 2012 IEEE AES Society's Barry Carlton Award for Best Paper published in IEEE Transactions on Aerospace and Electronic Systems, the 2003 IEE Achievement Award, and the 2003 IEEE AES Society Fred Nathanson Young Engineer of the Year award. He has authored or coauthored 11 book chapters, approximately 130 journal papers, and 170 conference papers.